

Splitting of elliptic flow in a tilted fireball

Tribhuban Parida* and Sandeep Chatterjee†

*Department of Physical Sciences,
Indian Institute of Science Education and Research Berhampur,
Transit Campus (Govt ITI),
Berhampur-760010, Odisha, India*

Abstract

The splitting of elliptic flow measured in different regions of the momentum space of produced hadrons has been recently studied in transport models and proposed as a sensitive probe of the angular momentum carried by the fireball produced in a relativistic heavy ion collision. The initial state angular momentum also gives rise to rapidity odd directed flow which has been measured. We consider a relativistic hydrodynamic framework with the initial matter distribution suitably calibrated to describe the observed directed flow and apply it to study the split in the elliptic flow. Our study suggests that the split in the elliptic flow is mostly driven by directed and triangular flows and may be used to constrain models of initial state rapidity distribution of matter in the fireball.

I. INTRODUCTION

The system of two non-central colliding relativistic heavy ion nuclei carries large angular momentum. In the aftermath of the collision, a part of this angular momentum is deposited in the locally thermalised fireball. The hydrodynamic response results in fluid vorticity and possibly spin polarisation which may be finally observed in the phase space occupation and polarisation states of the emitted particles [1–9].

There have been several attempts to model the initial longitudinal distribution of various hydrodynamic fields like the energy density and fluid velocity which after hydrodynamic evolution and particlization can leave their imprint on different observables [4, 6–26]. While for quite some time the rapidity dependence of directed flow has been used to discriminate such models of the initial three dimensional matter distribution [10, 11, 23–26], recently it has been demonstrated that even polarisation measurements of the final state hadrons can constrain such ansatz of initial matter distribution [24, 27].

It has been pointed out that the non-zero angular momentum of the fireball results in the splitting of elliptic flow in the momentum space of the final state hadrons [28]. This makes the splitting of elliptic flow a sensitive observable to constrain models of the initial state three dimensional matter distribution of the fireball. In a subsequent work, it was argued that this splitting is mainly driven by the directed flow [29]. These studies were conducted in a transport model framework and they don't describe the data on directed flow [30]. This raises concern on their model prediction of the elliptic flow splitting.

The various models of the longitudinal profile of the

fireball that has been explored so far can be broadly divided into two categories: shifted initial condition (SIC) [31] and tilted initial condition (TIC) [11]. In SIC, the rapidity profile at each point on the transverse plane is shifted according to the local centre of mass rapidity. TIC is inspired from the ansatz that a participant nucleon deposits more energy along its direction of motion [32–37]. It has been shown that SIC fails to describe the rapidity slope of directed flow at mid-rapidity in Au+Au at $\sqrt{s_{NN}} = 200$ GeV while TIC succeeds to describe the experimental data on directed flow, albeit with a free parameter η_m that parametrises the forward-backward asymmetry in the energy deposition of a participant in the initial state [11]. In this study, we discuss the contrasting nature of the splitting of the elliptic flow in different regions of the momentum space for both SIC as well as TIC, underlying the significance of this observable in our efforts to comprehend the longitudinal dynamics of the fireball.

II. INITIAL RAPIDITY PROFILE

We study Au+Au collisions at $\sqrt{s_{NN}} = 200$ GeV. The initial condition for the hydrodynamic evolution of the fireball is obtained from the Optical Glauber model. Here, the nucleus is modelled as a Woods-Saxon distribution $\rho(x, y, z) = \frac{\rho_0}{1 + \exp(\frac{r-R}{a})}$ where $r = \sqrt{x^2 + y^2 + z^2}$, $R = 6.38$ fm and $a = 0.535$ fm [38]. The z-axis is taken along the beam axis while the x-axis is along the impact parameter direction. The nuclear thickness function $T(x, y)$ is obtained as

$$T(x, y) = \int \rho(x, y, z) dz \quad (1)$$

using which one can define the total forward (N_+) and backward (N_-) going participants along the beam axis

* tribhubanp18@iiserbpr.ac.in

† sandeep@iiserbpr.ac.in

at a point (x, y) on the transverse plane

$$N_+(x, y) = T(x - b/2, y) (1 - (1 - \sigma_{NN} T(x + b/2, y))) \quad (2)$$

$$N_-(x, y) = T(x + b/2, y) (1 - (1 - \sigma_{NN} T(x - b/2, y))) \quad (3)$$

We have compared between two models of $\epsilon(x, y, \eta_s)$, the initial energy density deposited at a constant τ hypersurface at (x, y, η_s) : SIC [31] and TIC [11].

In case of SIC, the following ansatz is adopted for $\epsilon(x, y, \eta_s)$

$$\epsilon(x, y, \eta_s) = \epsilon_0 \left[(N_+(x, y) + N_-(x, y)) \frac{(1 - \alpha)}{2} + N_{coll}(x, y) \alpha \right] \times \epsilon_{\eta_s}(\eta_s - \eta_{sh}(x, y)) \quad (4)$$

where $\epsilon_{\eta_s}(\eta_s - \eta_{sh}(x, y))$ gives the η_s distribution at (x, y)

$$\epsilon_{\eta_s}(\eta_s) = \exp \left(-\frac{(|\eta_s| - \eta_0)^2}{2\sigma_\eta^2} \theta(|\eta_s| - \eta_0) \right) \quad (5)$$

We have used $\epsilon_0 = 13.2 \text{ GeV/fm}^3$, $\alpha = 0.14$, $\eta_0 = 1.3$ and $\sigma_\eta = 1.5$ that provides a good description of the $(\eta - \frac{dN_{ch}}{d\eta})$ data. $\eta_{sh}(x, y)$ is given by

$$\eta_{sh} = \frac{1}{2} \ln \frac{N_+(x, y) + N_-(x, y) + v_N(N_+(x, y) - N_-(x, y))}{N_+(x, y) + N_-(x, y) - v_N(N_+(x, y) - N_-(x, y))} \quad (6)$$

Here, v_N is the initial longitudinal velocity of each nucleon with mass m_N .

$$v_N = \sqrt{1 - (4m_N^2)/(s_{NN})} \quad (7)$$

The second initial condition that we have studied is the TIC. In this case $\epsilon(x, y, \eta_s)$ is given by

$$\epsilon(x, y, \eta_s) = \epsilon_0 [(N_+(x, y) f_+(\eta_s) + N_-(x, y) f_-(\eta_s)) \times (1 - \alpha) + N_{coll}(x, y) \epsilon_{\eta_s}(\eta_s) \alpha] \quad (8)$$

where $\epsilon_{\eta_s}(\eta_s)$ is the rapidity even profile as given in Eq. 5 and $f_{+,-}(\eta_s)$ introduce rapidity odd component in ϵ

$$f_{+,-}(\eta_s) = \epsilon_{\eta_s}(\eta_s) \epsilon_{F,B}(\eta_s) \quad (9)$$

where

$$\epsilon_F(\eta_s) = \begin{cases} 0, & \text{if } \eta_s < -\eta_m \\ \frac{\eta_s + \eta_m}{2\eta_m}, & \text{if } -\eta_m \leq \eta_s \leq \eta_m \\ 1, & \text{if } \eta_m < \eta_s \end{cases} \quad (10)$$

and

$$\epsilon_B(\eta_s) = \epsilon_F(-\eta_s) \quad (11)$$

We have used $\eta_m = 2.5$ to describe the directed flow data [30]. For both the initial conditions, we have assumed the Bjorken flow ansatz

$$u^\mu(\tau_0, x, y, \eta_s) = (\cosh \eta_s, 0, 0, \sinh \eta_s)$$

We evolve the above deposited initial energy distribution with the publicly available MUSIC code [39–42] which implements evolution within the framework of 3+1 D relativistic hydrodynamics followed by Cooper Frye freezeout at $T = 150 \text{ MeV}$ and finally allowing all the resonances to decay to stable hadrons under strong interaction. Thus, we obtain the momentum space probability distribution of hadrons using which we compute various observables. We consider the lattice QCD based equation of state, NEoS-B at zero baryon density [43–46] and take the shear viscosity η to entropy density s ratio, $\eta/s = 0.08$. We have ignored the effects of bulk viscosity.

III. SPLITTING OF THE ELLIPTIC FLOW

The azimuthal distribution of the hadrons in the plane transverse to the beam axis can be expanded into Fourier components in the following way:

$$\frac{dN}{d\phi} = \frac{1}{2\pi} \left(1 + 2 \sum_n (v_n \cos(n(\phi - \psi_{RP})) + s_n \sin(n(\phi - \psi_{RP}))) \right) \quad (12)$$

where ψ_{RP} is the reaction plane angle in the laboratory frame. v_n and s_n are the Fourier coefficients that characterise the distribution.

There has been a recent proposal to measure the split Δv_2 in $v_2 = \langle \cos(2(\phi - \psi_{RP})) \rangle$, as measured in different regions of the final hadron momentum space

$$\Delta v_2 = v_2^R - v_2^L \quad (13)$$

where $v_2^R = \langle \cos(2(\phi^R - \psi_{RP})) \rangle$ with $\phi^R \in ((\psi_{RP} - \pi/2), (\psi_{RP} + \pi/2))$ and $v_2^L = \langle \cos(2(\phi^L - \psi_{RP})) \rangle$ with $\phi^L \in ((\psi_{RP} + \pi/2), (\psi_{RP} + 3\pi/2))$. Here, $\langle \dots \rangle$ refers to averaging over the phase space of the produced hadrons.

ψ_{RP} is not directly measurable in experiments. The second order event plane orientation ψ_2 and the first order spectator plane ψ_{SP} have been proposed as good proxies for ψ_{RP} [47, 48]. However, for the determination of Δv_2 , ψ_{SP} alone is suitable as $\psi_2 = \pi$ is identified with $\psi_2 = 0$ and hence does not distinguish between the phase spaces associated with ϕ^R and ϕ^L . Recently, the Event Plane Detector has been installed at large rapidities which can also be used to estimate ψ_{RP} [49].

v_2^R and v_2^L work out to be the following [29]:

$$v_2^R = \frac{\int_{\psi_{\text{RP}} - \frac{\pi}{2}}^{\psi_{\text{RP}} + \frac{\pi}{2}} \cos(2(\phi - \psi_{\text{RP}})) \frac{dN}{d\phi} d\phi}{\int_{\psi_{\text{RP}} - \frac{\pi}{2}}^{\psi_{\text{RP}} + \frac{\pi}{2}} \frac{dN}{d\phi} d\phi} \approx \frac{v_2 + \frac{4v_1}{3\pi} + \frac{12v_3}{5\pi} - \frac{20v_5}{21\pi}}{1 + \frac{4v_1}{\pi} - \frac{4v_3}{3\pi} + \frac{4v_5}{5\pi}} \quad (14)$$

$$v_2^L = \frac{\int_{\psi_{\text{RP}} + \frac{\pi}{2}}^{\psi_{\text{RP}} + \frac{3\pi}{2}} \cos(2(\phi - \psi_{\text{RP}})) \frac{dN}{d\phi} d\phi}{\int_{\psi_{\text{RP}} + \frac{\pi}{2}}^{\psi_{\text{RP}} + \frac{3\pi}{2}} \frac{dN}{d\phi} d\phi} \approx \frac{v_2 - \frac{4v_1}{3\pi} - \frac{12v_3}{5\pi} + \frac{20v_5}{21\pi}}{1 - \frac{4v_1}{\pi} + \frac{4v_3}{3\pi} - \frac{4v_5}{5\pi}} \quad (15)$$

In Eqs. 14 and 15 we have omitted contributions from harmonics higher than the fifth order. Further, from Eqs. 13, 14 and 15 we get

$$\Delta v_2 \approx \frac{8v_1}{3\pi} + \frac{24v_3}{5\pi} - \frac{40v_5}{21\pi} \quad (16)$$

In Eq. 16 only terms which are linear in the flow harmonics have been shown as they are sufficient to estimate Δv_2 . Thus, Δv_2 is sourced mainly by the odd flow harmonics. The collision geometry is such that these odd flow harmonics have rapidity odd components with respect to the reaction plane. Hence, Δv_2 is also rapidity odd following the odd flow harmonics which is also evident from Eq. 13. There has been measurement of directed flow with respect to ψ_{SP} [30]. Optical Glauber model with TIC followed by hydrodynamic expansion is able to describe the v_1 measurement at $\sqrt{s_{\text{NN}}} = 200$ GeV for Au+Au collisions[11]. Here, we use similar TIC within an optical Glauber model followed by hydrodynamic expansion to compute the model expectation for Δv_2 . We expect similar results on including fluctuations in the initial condition [50].

IV. RESULTS

We will now present the prediction for Δv_2 with respect to the reaction plane as computed with TIC as well as SIC. As seen in Eq. 16, the leading contributions to Δv_2 arise from the odd harmonics, out of which there are STAR measurements on v_1 with respect to the spectator plane [30]. Thus, we first compare the model results with the STAR data for v_1 in Fig. 1. We have plotted the model expectations for $v_1 - \eta$ and $v_1 - p_T$ in the panels (a) and (b) respectively and compared them to the STAR measurements [30]. The model results have been shown for both TIC (red solid line) as well as those from SIC (dashed blue line). We find that for both $v_1 - \eta$ and $v_1 - p_T$, TIC is able to describe the STAR data

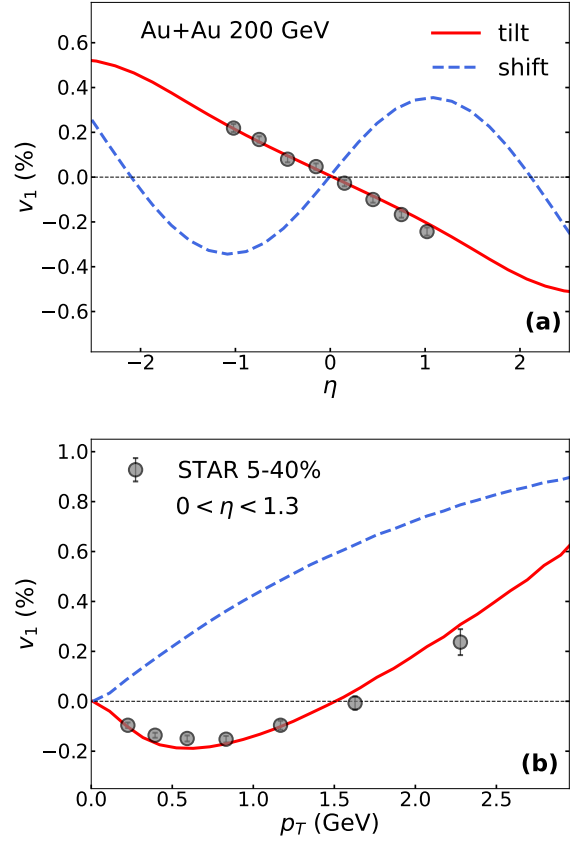


FIG. 1. (Color online) Phase space dependence of v_1 is computed both for tilted initial condition (red solid line) and shifted initial condition (blue dashed line) for 5-40 % centrality Au+Au collisions at $\sqrt{s_{\text{NN}}} = 200$ GeV. The model expectations are compared to measurements from the STAR collaboration [30]. v_1 vs η is shown in panel (a) and v_1 vs p_T is shown in panel (b).

well while SIC fails. This is in agreement with earlier studies [11, 26]. Thus, we expect TIC to provide correct prediction of Δv_2 .

The good description of v_1 by TIC motivates us further to compute Δv_2 vs η within the same scheme. In Fig. 2 we have shown the model predictions for the η dependence of Δv_2 . Further, we have also plotted the odd harmonics along with appropriate coefficients as suggested by Eq. 16 that are the dominant contributors to Δv_2 . Firstly, we note that Δv_2 arises as a competition between $\frac{8v_1}{3\pi}$ and $\frac{24v_3}{5\pi}$ as they are of opposite signs. The $\frac{8v_1}{3\pi}$ term marginally wins and hence Δv_2 follows its sign. For $|\eta| < 1$, $\Delta v_2 \sim 10^{-4}$ and it grows substantially for larger η . The contribution from v_5 is negligible in the entire η range.

The p_T dependence is shown in Fig. 3. The predictions for $0 < \eta < 1.3$ and $1.3 < \eta < 2.5$ are shown separately

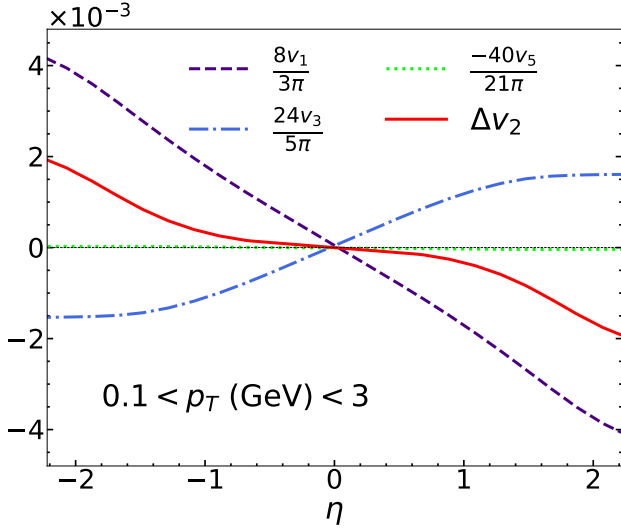


FIG. 2. (Color online) The prediction for Δv_2 vs η with tilt initial condition has been plotted in red solid line. Further, the first three leading flow harmonics that contribute to Δv_2 (see Eq. 16) are shown as well.

in panels (a) and (b) respectively. As expected from the η dependence, the magnitude of the split is larger in the $1.3 < \eta < 2.5$, otherwise, the trends are similar. Δv_2 is negative for small p_T . There is a turning point around $p_T \sim 0.4$ GeV after which it crosses zero at $p_T \sim 1$ GeV and monotonically rises. This p_T dependence of Δv_2 is mainly borrowed from v_1 which also has a similar trend unlike v_3 which remains positive for all p_T . It is interesting to note that for $p_T > 1.5$ GeV, v_3 becomes the dominant contributor.

Further, we present a comparative study of Δv_2 computed with TIC and SIC in Fig. 4. The results on the η dependence of Δv_2 are presented in panel (a) while the p_T dependence is plotted in panel (b). As seen in panel (a), for $|\eta| < 1$, Δv_2 is around 10-20 times larger in SIC as compared to TIC. Further they are of opposite signs—at positive rapidities while the SIC gives a positive Δv_2 , the TIC yields a negative Δv_2 . This may be traced to the fact that v_1 is of opposite sign in the two models. Further, from panel (b) we note that the origin of this opposite sign is from the low p_T region as for $p_T > 1.5$ GeV, both models yield positive values. While we noted earlier that Δv_2 results out of tension between v_1 and v_3 in the TIC, in the SIC we find that it is mostly controlled by v_1 as v_3 turns out to be small in this case. It is worth noting here that an earlier study of Δv_2 within the transport framework of the AMPT model had similar conclusions as the results here with SIC [29]. Thus, the characteristics of Δv_2 can serve as a sensitive probe of rapidity dependent initial condition of the fireball.

It is well known that the various model systematics of

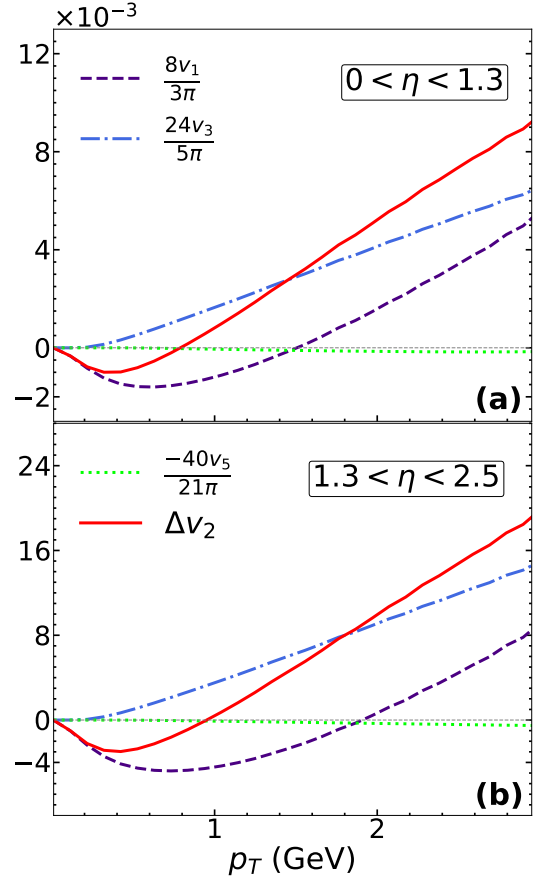


FIG. 3. (Color online) The prediction for Δv_2 vs p_T with tilt initial condition has been plotted in red solid line. Further, the first three leading flow harmonics that contribute to Δv_2 (see Eq. 16) are shown as well.

the transverse initial condition can result in the variation of v_2 [51–53]. Such model dependencies can creep into our predictions of Δv_2 as well. We suggest to scale Δv_2 with v_2 in order to cancel out such systematics of the transverse initial condition which are not of interest here. We present the results of Δv_2 scaled by v_2 in Fig. 5. The η dependence is plotted in panel (a). $|\Delta v_2/v_2|$ stays below 0.005 for $|\eta| < 1$ beyond which it has a rapid linear growth. The p_T differential values are plotted in panel (b). We obtain about 3% and 5% $\Delta v_2/v_2$ at $p_T \sim 1.5$ GeV for $0 < \eta < 1.3$ and $1.3 < \eta < 2.5$ respectively. The ratio of phase space integrated Δv_2 and v_2 , $\Delta v_2/v_2$ comes out to be -0.0019 and -0.0268 for $0 < \eta < 1.3$ and $1.3 < \eta < 2.5$ respectively.

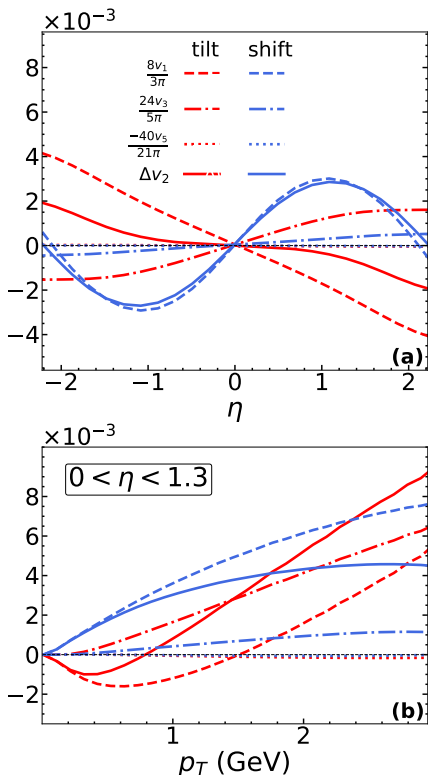


FIG. 4. (Color online) The predictions for phase space dependence of Δv_2 has been compared between tilt initial condition and shift initial condition. Further, the first three leading flow harmonics that contribute to Δv_2 are also shown for each model to understand the origin in the difference of their phase space dependence of Δv_2 . Δv_2 vs η is shown in panel (a) and Δv_2 vs p_T is shown in panel (b).

V. SUMMARY

The collision geometry of a non-central relativistic heavy ion collision introduces a large angular momentum in its initial state. Rapidity odd directed flow is a natural consequence of this. Such observables probe the longitudinal profile of the fireball. Recently, it has been observed that such large angular momentum in the initial state also causes a split in the magnitude of v_2 , Δv_2 in different regions of the final state hadron momentum space - parallel and anti-parallel to the impact parameter direction [28, 29]. Δv_2 has been proposed to be a sensitive probe of the initial rapidity profile of the fireball. A transport model framework was adopted in these works that do not describe the v_1 data.

In this work, we have revisited the estimation of Δv_2 within a 3+1 D relativistic hydrodynamic framework with tilted initial condition that is known to describe the v_1 data [11]. We find v_1 to be the leading contributor to Δv_2 , as was reported in earlier studies. However, unlike

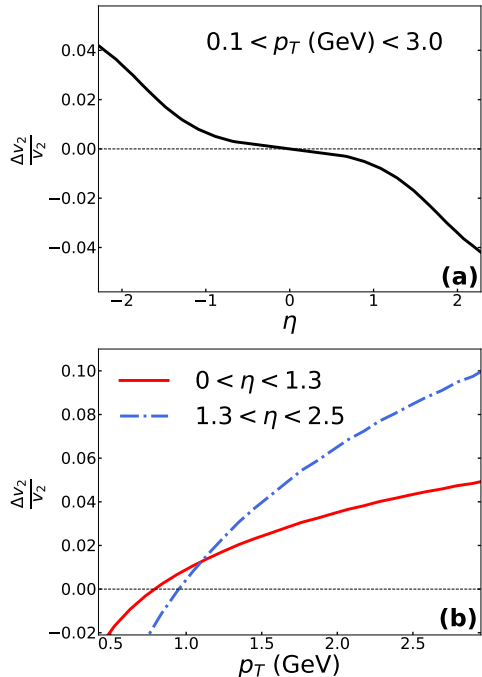


FIG. 5. (Color online) The predictions for phase space dependence of $\Delta v_2/v_2$ has been shown for tilt initial condition. Panel (a) shows the η dependence while panel (b) shows the p_T dependence.

in those transport model based studies, we find that the tilted initial condition gives rise to sizeable rapidity odd v_3 which also contributes significantly to Δv_2 , particularly for $p_T > 1.5$ GeV, it becomes the dominant contributor to Δv_2 . In order to demonstrate the sensitivity of Δv_2 to the choice of the initial condition, we have computed Δv_2 also with shifted initial condition. In this case, similar to the earlier studies, v_3 comes out to be negligible and hence Δv_2 gets contribution dominantly from v_1 . The η dependence of Δv_2 is of opposite sign for titled versus shifted initial conditions owing to the opposite signs of their v_1 . Finally, we have also presented the ratio of Δv_2 to v_2 so as to get rid of the various model uncertainties that affect v_2 and hence also Δv_2 : for $p_T \sim 1.5$ GeV we obtain $\Delta v_2/v_2 \sim 3\%$ and 5% for $0 < \eta < 1.3$ and $1.3 < \eta < 2.5$ respectively. Our study demonstrates that Δv_2 can play complementary role to v_1 in constraining the rapidity profile of the fireball.

VI. ACKNOWLEDGEMENTS

SC acknowledges helpful discussions with Piotr Bozek and IISER Berhampur for Seed Grant.

-
- [1] Z.-T. Liang and X.-N. Wang, Phys. Rev. Lett. **94**, 102301 (2005), [Erratum: Phys.Rev.Lett. 96, 039901 (2006)], arXiv:nucl-th/0410079.
- [2] Z.-T. Liang and X.-N. Wang, Phys. Lett. B **629**, 20 (2005), arXiv:nucl-th/0411101.
- [3] F. Becattini, F. Piccinini, and J. Rizzo, Phys. Rev. C **77**, 024906 (2008), arXiv:0711.1253 [nucl-th].
- [4] B. Betz, M. Gyulassy, and G. Torrieri, Phys. Rev. C **76**, 044901 (2007), arXiv:0708.0035 [nucl-th].
- [5] A. Ipp, A. Di Piazza, J. Evers, and C. H. Keitel, Phys. Lett. B **666**, 315 (2008), arXiv:0710.5700 [hep-ph].
- [6] F. Becattini, L. Csernai, and D. J. Wang, Phys. Rev. C **88**, 034905 (2013), [Erratum: Phys.Rev.C 93, 069901 (2016)], arXiv:1304.4427 [nucl-th].
- [7] F. Becattini, G. Inghirami, V. Rolando, A. Beraudo, L. Del Zanna, A. De Pace, M. Nardi, G. Pagliara, and V. Chandra, Eur. Phys. J. C **75**, 406 (2015), [Erratum: Eur.Phys.J.C 78, 354 (2018)], arXiv:1501.04468 [nucl-th].
- [8] L.-G. Pang, H. Petersen, Q. Wang, and X.-N. Wang, Phys. Rev. Lett. **117**, 192301 (2016), arXiv:1605.04024 [hep-ph].
- [9] I. Karpenko and F. Becattini, Eur. Phys. J. C **77**, 213 (2017), arXiv:1610.04717 [nucl-th].
- [10] R. J. M. Snellings, H. Sorge, S. A. Voloshin, F. Q. Wang, and N. Xu, Phys. Rev. Lett. **84**, 2803 (2000), arXiv:nucl-ex/9908001.
- [11] P. Bozek and I. Wykiel, Phys. Rev. C **81**, 054902 (2010), arXiv:1002.4999 [nucl-th].
- [12] P. Bozek, W. Broniowski, and J. Moreira, Phys. Rev. C **83**, 034911 (2011), arXiv:1011.3354 [nucl-th].
- [13] P. Bozek, W. Broniowski, and A. Olszewski, Phys. Rev. C **91**, 054912 (2015), arXiv:1503.07425 [nucl-th].
- [14] P. Bozek and W. Broniowski, Phys. Lett. B **752**, 206 (2016), arXiv:1506.02817 [nucl-th].
- [15] P. Bozek, W. Broniowski, and A. Olszewski, Phys. Rev. C **92**, 054913 (2015), arXiv:1509.04124 [nucl-th].
- [16] W. Broniowski and P. Bozek, Phys. Rev. C **93**, 064910 (2016), arXiv:1512.01945 [nucl-th].
- [17] S. Chatterjee and P. Bozek, Phys. Rev. C **96**, 014906 (2017), arXiv:1704.02777 [nucl-th].
- [18] P. Bozek and W. Broniowski, Phys. Rev. C **97**, 034913 (2018), arXiv:1711.03325 [nucl-th].
- [19] L.-G. Pang, H. Petersen, G.-Y. Qin, V. Roy, and X.-N. Wang, Eur. Phys. J. A **52**, 97 (2016), arXiv:1511.04131 [nucl-th].
- [20] L.-G. Pang, G.-Y. Qin, V. Roy, X.-N. Wang, and G.-L. Ma, Phys. Rev. C **91**, 044904 (2015), arXiv:1410.8690 [nucl-th].
- [21] L.-G. Pang, H. Petersen, and X.-N. Wang, Phys. Rev. C **97**, 064918 (2018), arXiv:1802.04449 [nucl-th].
- [22] X.-Y. Wu, L.-G. Pang, G.-Y. Qin, and X.-N. Wang, Phys. Rev. C **98**, 024913 (2018), arXiv:1805.03762 [nucl-th].
- [23] C. Shen and S. Alzhirani, Phys. Rev. C **102**, 014909 (2020), arXiv:2003.05852 [nucl-th].
- [24] S. Ryu, V. Jovic, and C. Shen, Phys. Rev. C **104**, 054908 (2021), arXiv:2106.08125 [nucl-th].
- [25] Z.-F. Jiang, C. B. Yang, and Q. Peng, (2021), 10.1103/PhysRevC.104.064903, arXiv:2111.01994 [hep-ph].
- [26] Z.-F. Jiang, S. Cao, X.-Y. Wu, C. B. Yang, and B.-W. Zhang, Phys. Rev. C **105**, 034901 (2022), arXiv:2112.01916 [hep-ph].
- [27] S. Alzhirani, S. Ryu, and C. Shen, (2022), arXiv:2203.15718 [nucl-th].
- [28] Z. Chen, Z. Wang, C. Greiner, and Z. Xu, (2021), arXiv:2108.12735 [hep-ph].
- [29] C. Zhang and Z.-W. Lin, (2021), arXiv:2109.04987 [nucl-th].
- [30] B. I. Abelev et al. (STAR), Phys. Rev. Lett. **101**, 252301 (2008), arXiv:0807.1518 [nucl-ex].
- [31] T. Hirano and K. Tsuda, Phys. Rev. C **66**, 054905 (2002), arXiv:nucl-th/0205043.
- [32] S. J. Brodsky, J. F. Gunion, and J. H. Kuhn, Phys. Rev. Lett. **39**, 1120 (1977).
- [33] B. B. Back et al., Phys. Rev. Lett. **91**, 052303 (2003), arXiv:nucl-ex/0210015.
- [34] A. Bialas and W. Czyz, Acta Phys. Polon. B **36**, 905 (2005), arXiv:hep-ph/0410265.
- [35] A. Adil and M. Gyulassy, Phys. Rev. C **72**, 034907 (2005), arXiv:nucl-th/0505004.
- [36] N. Armesto, L. McLerran, and C. Pajares, Nucl. Phys. A **781**, 201 (2007), arXiv:hep-ph/0607345.
- [37] A. Bzdak and K. Wozniak, Phys. Rev. C **81**, 034908 (2010), arXiv:0911.4696 [hep-ph].
- [38] Q. Y. Shou, Y. G. Ma, P. Sorensen, A. H. Tang, F. Videbæk, and H. Wang, Phys. Lett. B **749**, 215 (2015), arXiv:1409.8375 [nucl-th].
- [39] B. Schenke, S. Jeon, and C. Gale, Phys. Rev. C **82**, 014903 (2010), arXiv:1004.1408 [hep-ph].
- [40] B. Schenke, S. Jeon, and C. Gale, Phys. Rev. C **85**, 024901 (2012), arXiv:1109.6289 [hep-ph].
- [41] G. S. Denicol, C. Gale, S. Jeon, A. Monnai, B. Schenke, and C. Shen, Phys. Rev. C **98**, 034916 (2018), arXiv:1804.10557 [nucl-th].
- [42] J.-F. Paquet, C. Shen, G. S. Denicol, M. Luzum, B. Schenke, S. Jeon, and C. Gale, Phys. Rev. C **93**, 044906 (2016), arXiv:1509.06738 [hep-ph].
- [43] A. Monnai, B. Schenke, and C. Shen, Phys. Rev. C **100**, 024907 (2019), arXiv:1902.05095 [nucl-th].
- [44] A. Bazavov et al. (HotQCD), Phys. Rev. D **90**, 094503 (2014), arXiv:1407.6387 [hep-lat].
- [45] A. Bazavov et al. (HotQCD), Phys. Rev. D **86**, 034509 (2012), arXiv:1203.0784 [hep-lat].
- [46] H. T. Ding, S. Mukherjee, H. Ohno, P. Petreczky, and H. P. Schadler, Phys. Rev. D **92**, 074043 (2015), arXiv:1507.06637 [hep-lat].
- [47] L. Adamczyk et al. (STAR), Phys. Rev. C **88**, 064911 (2013), arXiv:1302.3802 [nucl-ex].
- [48] B. Abelev et al. (ALICE), Phys. Rev. Lett. **110**, 012301 (2013), arXiv:1207.0900 [nucl-ex].
- [49] J. Adams et al., Nucl. Instrum. Meth. A **968**, 163970 (2020), arXiv:1912.05243 [physics.ins-det].
- [50] P. Bozek, Phys. Rev. C **85**, 034901 (2012), arXiv:1110.6742 [nucl-th].

- [51] C. Shen, S. A. Bass, T. Hirano, P. Huovinen, Z. Qiu, H. Song, and U. Heinz, *J. Phys. G* **38**, 124045 (2011), arXiv:1106.6350 [nucl-th].
- [52] Z. Qiu and U. W. Heinz, *Phys. Rev. C* **84**, 024911 (2011), arXiv:1104.0650 [nucl-th].
- [53] M. Ruggieri, F. Scardina, S. Plumari, and V. Greco, *Phys. Lett. B* **727**, 177 (2013), arXiv:1303.3178 [nucl-th].